


RESEARCH ARTICLE

OCT4/POU5F1 is indispensable for the lineage differentiation of the inner cell mass in bovine embryos

Kilian Simmet^{1,2}  | Mayuko Kurome^{1,2} | Valeri Zakhartchenko^{1,2} |
 Horst-Dieter Reichenbach³ | Claudia Springer^{1,2} | Andrea Bähr^{1,2} | Helmut Blum⁴ |
 Julia Philippou-Massier⁴ | Eckhard Wolf^{1,2,3} 

¹Gene Center, Department of Veterinary Sciences, Institute of Molecular Animal Breeding and Biotechnology, LMU Munich, Munich, Germany

²Center for Innovative Medical Models (CiMM), LMU Munich, Oberschleißheim, Germany

³Bavarian State Research Center for Agriculture, Institute of Animal Breeding, Poing, Germany

⁴Laboratory for Functional Genome Analysis (LAFUGA), Gene Center, LMU Munich, Munich, Germany

Correspondence

Kilian Simmet, Hackerstrasse 27, 85764 Oberschleißheim, Germany.
 Email: k.simmet@gen.vetmed.uni-muenchen.de

Present address

Andrea Bähr, Internal Medicine I, Klinikum rechts der Isar, TU Munich, Munich, Germany

Funding information

This work was supported by funds from the Deutsche Forschungsgemeinschaft (DFG) under grants 405453332 and TRR127 and from the Bayerische Forschungsförderung under grant AZ-1300-17.

Abstract

The mammalian blastocyst undergoes two lineage segregations, that is, formation of the trophectoderm and subsequently differentiation of the hypoblast (HB) from the inner cell mass, leaving the epiblast (EPI) as the remaining pluripotent lineage. To clarify the expression patterns of markers specific for these lineages in bovine embryos, we analyzed day 7, 9, and 12 blastocysts completely produced in vivo by staining for OCT4, NANOG, SOX2 (EPI), and GATA6, SOX17 (HB) and identified genes specific for these developmental stages in a global transcriptomics approach. To study the role of OCT4, we generated OCT4-deficient (*OCT4* KO) embryos via somatic cell nuclear transfer or in vitro fertilization. *OCT4* KO embryos reached the expanded blastocyst stage by day 8 but lost NANOG and SOX17 expression, while SOX2 and GATA6 were unaffected. Blastocysts transferred to recipient cows from day 6 to 9 expanded, but the *OCT4* KO phenotype was not rescued by the uterine environment. Exposure of *OCT4* KO embryos to exogenous FGF4 or chimeric complementation with *OCT4* intact embryos did not restore NANOG or SOX17 in *OCT4*-deficient cells. Our data show that OCT4 is required cell autonomously for the maintenance of pluripotency of the EPI and differentiation of the HB in bovine embryos.

KEYWORDS

bovine, differentiation, embryo, pluripotency

Abbreviations: AI, artificial insemination; DAPI, 4',6-diamidino-2-phenylindole; DAT, differentially abundant transcript; EPI, epiblast; FSC, fetal somatic cells; HB, hypoblast; ICM, inner cell mass; IVF, in vitro fertilization; KO, knockout; *OCT4* KO, *OCT4*-deficient; PE, primitive endoderm; PFA, paraformaldehyde; RL, Rauber's layer; RNP, ribonucleoprotein; SCNT, somatic cell nuclear transfer; SD, standard deviation; TE, trophectoderm; ZI, zygote injection; ZP, zona pellucida.

This is an open access article under the terms of the [Creative Commons Attribution](https://creativecommons.org/licenses/by/4.0/) License, which permits use, distribution and reproduction in any medium, provided the original work is properly cited.

© 2022 The Authors. *The FASEB Journal* published by Wiley Periodicals LLC on behalf of Federation of American Societies for Experimental Biology

1 | INTRODUCTION

During preimplantation development, the mammalian embryo undergoes two consecutive lineage differentiations resulting in a blastocyst with three distinct lineages. The trophectoderm (TE) represents the first differentiated epithelium and envelopes the inner cell mass (ICM), which retains a pluripotent state. Subsequently, within the ICM, the primitive endoderm (PE) or hypoblast (HB) in human and bovine segregates from the epiblast (EPI), which contains the last pluripotent cells and gives rise to the embryo proper. The TE will contribute the embryonic portion of the placenta and the PE/HB develops into the yolk sac.^{1,2} The fundamental mechanisms regulating these events have been studied extensively in the mouse, while advances in genome editing have enabled researchers to study the specific function of genes during preimplantation development in alternative model organisms. Given the substantial differences in the regulation of lineage differentiation and the maintenance of pluripotency between mouse and other mammalian species, this progress harbors the prospect of a deeper understanding of preimplantation development, also in human. Because in vitro embryo production techniques are highly advanced in bovine, this species offers great opportunities as a model for preimplantation development.^{3–5}

The second lineage differentiation, when the PE/HB and EPI segregate, is regulated by EPI precursor cells expressing FGF4, which via the MEK-pathway induces the differentiation of PE/HB precursor cells. Preimplantation embryos cultured with exogenous FGF4 develop an ICM entirely made up of PE/HB cells.⁴ The transcription factor OCT4/POU5F1 plays a pivotal role in mammalian embryo development, as it regulates both the maintenance of pluripotency as well as differentiation events.⁶ In mouse, loss of OCT4 prevents the development of the PE during the second lineage differentiation, while initial expression of the EPI marker NANOG is not affected.^{7,8} On the contrary, the expression of NANOG fails in OCT4-deficient bovine blastocysts, while the early presumptive HB marker GATA6 is still present. Yet, it remains unclear if OCT4 has a role in the second lineage differentiation in bovine embryos, as GATA6 does not exclusively mark cells committed to the HB, but also cells in the TE.^{9,10}

Because data on the second lineage differentiation in bovine embryos are scarce, we first investigated expression patterns of lineage marker proteins and transcriptome dynamics of day 7, 9, and 12 embryos produced completely in vivo (thus representing bona fide samples of early bovine development). Studies of *OCT4* knockout (KO) blastocysts generated by somatic cell nuclear transfer (SCNT) and zygote injection (ZI) showed that both EPI maintenance and HB differentiation are dependent on OCT4. Neither chimeric complementation with *OCT4*-intact blastomeres nor supplementation of exogenous FGF4 could rescue the

OCT4 KO phenotype. Therefore, we conclude that—as in mouse—OCT4 is required cell autonomously during the differentiation of the HB in bovine blastocysts.

2 | MATERIALS AND METHODS

2.1 | Ethics statement

All animal procedures in this study were performed according to the German Animal Welfare Act and to a protocol approved by the Regierung von Oberbayern (reference number ROB-55.2-2532.Vet_02-20-73).

2.2 | Statistics

All data were analyzed with GraphPad Prism 5.04, mean values \pm standard deviation (SD) are presented. Statistical tests were two-tailed unpaired *t* test for pairwise comparisons or one-way ANOVA with Tukey multiple comparison test for analyses with more experimental groups. Level of significance was set to $p < .05$.

2.3 | Superstimulation of donors, transfer, and flushing of in vivo produced embryos

German Simmental heifers, 18–20 months old and 350–420 kg, served as embryo donors and recipients. Superstimulation and artificial insemination (AI) were performed as described previously³⁴ and the embryos were collected nonsurgically by flushing at day 7, 9, or 12 (day 0 = estrus) using a flushing catheter with an enlarged tip-opening. For transfer of day 6 in vitro produced embryos to the uterus, the estrous cycle of recipient heifers was synchronized with a progesterone-releasing intravaginal device for 8 days (PRID-alpha, Ceva) and a single dose of PGF2 α analog (500 μ g cloprostenol, Estrumate, Essex) at removal of the PRID. After 48–72 h, the recipients showed signs of estrus. At day 6, embryos were transferred using a standard procedure³⁵ and collected at day 9 as described above.

2.4 | RNA-sequencing and data analysis

The generation of RNA-sequencing libraries, sequencing, and data analysis was performed as described previously.⁹ Briefly, after isolation of RNA, cDNA and RNA sequencing libraries were generated using the Ovation RNA-Seq System V2 Kit (Tecan Genomics) and tagmentation technology of the Nextera XT kit (Illumina), respectively.

Libraries were sequenced on a HiSeq1500 machine (Illumina) and reads were mapped to the bovine reference genome *ARS-UCD1.2*¹⁸ with STAR RNA sequence read mapper.³⁶ Differential gene expression analysis was performed with DeSeq2³⁷; heat map was generated from a mean-centered matrix using Heatmapper.³⁸

2.5 | In vitro fertilization and somatic cell nuclear transfer procedures

In vitro fertilization and SCNT were performed as described previously.³⁹ Presumptive zygotes and activated fused complexes from SCNT were cultured in synthetic oviductal fluid supplemented with 5% estrous cow serum, 2× of basal medium Eagle's amino acid solution 50× (Merck), and 1× of minimal essential medium nonessential amino acid solution 100× (Merck). For culture of embryos with exogenous FGF4, human recombinant FGF4 (R&D Systems) and heparin (Merck) were added at 1 μg/ml each.²⁵

2.6 | Immunofluorescence microscopy and image analysis

Before fixation, the zona pellucida (ZP) was removed enzymatically using pronase (Merck)⁴⁰ or mechanically for in vitro produced or flushed embryos, respectively. Embryos from in vitro culture were fixed in a solution containing 2% paraformaldehyde (PFA, Merck) for 20 min at 37°C⁴¹ and flushed embryos were fixed in 4% PFA overnight at 4°C. After sequential blocking for each 1 h in 5% donkey and fetal calf serum (Jackson Immunoresearch) and 0.5% Triton X-100 (Merck), embryos were transferred to the first antibody solution and incubated overnight at 4°C. After washing, embryos were incubated in the second antibody solution for 1 h at 37°C and subsequently mounted in Vectashield mounting medium containing 4',6-diamidino-2-phenylindole (DAPI, Vector Laboratories) in a manner that conserves the 3D structure of the specimen.⁴² The antibodies used and their dilutions are provided in Table S1. Stacks of optical sections were recorded with a Leica SP8 confocal microscope (Leica) at an interval of 1 μm using water immersion HC PL APO CS2 40X 1.1 NA or HC PL APO CS2 20X 0.75 NA objectives (Leica) and a pinhole of 0.9 airy units. DAPI, eGFP, Alexa Fluor 555, Rhodamine Red™-X, and Alexa Fluor 647 were excited with laser lines of 405, 488, 499, 573, and 653 nm, respectively, and detection ranges were set to 422–489 nm, 493–616 nm, 561–594 nm, 578–648 nm, and 660–789 nm, respectively. Cell numbers were counted manually using the manual counting plug-in of Icy bio-imaging software,⁴³ figures were produced using FigureJ software.⁴⁴

2.7 | Induction of *OCT4* knockout in fibroblast cells and zygotes

For the transfection of female adult ear fibroblasts, sgRNA2b (5'-ACTCACCAAAGAGAACCCCC-3') was cloned into pSpCas9(BB)-2A-Puro (PX459) V2.0, a gift from Feng Zhang (Addgene plasmid #62988), using the *BbsI* cutting site.²² Transfection and clonal expansion after selection with 2 μg/ml puromycin for 48 h were performed as described previously.⁴⁵ The generation of *OCT4* KO cells randomly tagged by eGFP was achieved by first transfecting somatic cells derived from a male fetus with a crown-rump length of 9 cm (FSC) with a linearized DNA construct and subsequently inducing *OCT4* KO via lipofection using a ribonucleoprotein (RNP) containing the sgRNA2b. The linearized construct was produced by excising the CAG-eGFP-SV40pA sequence from a plasmid, generated by introducing a de novo synthesized CAG promoter and eGFP-SV40pA⁴⁶ into the pUC57-AmpR vector backbone. The RNP was produced by mixing the synthetic and modified sgRNA2b (Synthego) and TrueCut™ Cas9 Protein v2 (Thermo Fisher Scientific) at equimolar concentrations of 8 μM in 10 mM Tris-buffer with 1 mM EDTA. Lipofection was performed in a six-well dish using CRISPRMAX™ Cas9 Transfection Reagent (Thermo Fisher Scientific) according to the manufacturer's instructions. After 48 h of lipofection, eGFP-positive cells were sorted individually into 96-well dishes and clonally expanded as described above. Screening of single-cell clones for mutations at *OCT4* and *ETF1* was achieved by Sanger sequencing as described previously⁹ with primers presented in Table S2. For ZI, RNPs with final concentrations of 2 μM sgRNA2b or sgRNA Ctrl (5'-GGTCTTCGAGAAGACCTGCG-3') and 1 μM Cas9 in 10 mM Tris-buffer with 0.1 mM EDTA were produced as described above. After co-incubation of sperm and cumulus-oocyte complexes for 14 h, cumulus cells were removed by vortexing and approximately 10 pl of the RNP was injected into presumptive zygotes using a FemtoJet4i device (Eppendorf). After 7 days of culture, DNA was extracted by incubating the blastocysts in a buffer containing 25 mM MgCl₂, 1 μl/ml TritonX-100, and 150 μg/ml Proteinase K (Carl Roth) at 37°C for 1 h and subsequently at 99°C for 8 min. For Sanger sequencing, a nested PCR amplification of the *OCT4* locus was performed using 2 μl of the DNA extraction buffer directly as template. For the first PCR, we ran 25 cycles with Herculase II Fusion DNA Polymerase (Agilent) in a 25 μl reaction volume; the second PCR used 2 μl of the first reaction as template and HotStarTaq DNA Polymerase (Qiagen) in a 20 μl reaction volume for 15 cycles. All PCRs were performed using the buffers and instructions provided by the manufacturers; primer sequences are provided in Table S2. Extraction of

DNA from fixed embryos after the imaging procedure was achieved by using the QIAamp DNA Micro Kit (Qiagen) according to the manufacturer's instructions regarding the isolation of genomic DNA from laser-microdissected tissues followed by 35 cycles of Herculanase II PCR using 4 μ l of template.

2.8 | Chimera aggregation

Embryos were produced via SCNT from *OCT4* KO cells tagged with eGFP (*OCT4*^{2bKOeGFP}) and FSC wild-type cells (NT Ctrl^{FSC}). At day 4, the ZP was removed enzymatically and each one morula from *OCT4*^{2bKOeGFP} and NT Ctrl^{FSC} were aggregated to a chimera using phytohemagglutinin (Merck) and cultured as described previously.⁴⁰ Chimera formation was confirmed by time-lapse imaging (Primo Vision, Vitrolife) and by detection of both eGFP-positive and -negative cells in the developed blastocysts. Chimeric blastocysts were fixed and stained as described above.

3 | RESULTS

3.1 | Lineage marker and transcriptome dynamics during the second lineage differentiation of in vivo produced embryos

To investigate the expression patterns of lineage markers of EPI (*OCT4*, *NANOG*, *SOX2*) and HB (*SOX17*, *GATA6*), we stained embryos flushed from the uterus after superstimulation as bona fide samples at days 7, 9, and 12 from $n = 7$ (day 7 and 9) and $n = 3$ (day 12) different donor cows. At day 7, *OCT4* was present in the ICM (Figure 1) and in the TE (Figure S1), and by day 9, *OCT4* was restricted to EPI cells and the percentage of *OCT4* cells strongly decreased. At all examined stages, *NANOG* was only present in EPI cells and their precursors, that is, co-expressed with *OCT4* and *SOX2* but mutually exclusive with *GATA6* and *SOX17*. *SOX2* was expressed pan-ICM at day 7 and restricted to EPI by day 9, resulting in a decreased percentage of *SOX2*-positive cells. Together with *NANOG*, *SOX2* cells were still present in the embryonic disk at day 12 and it has been shown previously that *OCT4* is present in this lineage until day 17.^{11,12} A total of 28 day 7 blastocysts were stained against *SOX17*, where this transcription factor was not present in eight embryos and only faint and restricted to the ICM in the remainder. By day 9, the HB began to form an inner lining of the blastocoel cavity consisting of the visceral and parietal HB,^{13,14} which were both marked by *SOX17* until day 12. *GATA6* was expressed at day 7 and 9 in the TE and ICM,

but not co-expressed with *NANOG*. At day 12, there was no *GATA6* visible in any of the lineages (Figure 1).

In a global transcriptomics approach, we aimed to identify genes that are specific to the developmental stages at day 7, 9, and 12 and the respective embryonic cell lineages EPI, HB, and TE. From three different donor cows, we analyzed three day 7 and each four day 9 and day 12 embryos. Differential gene expression analysis using DESeq2 revealed 1890 and 2716 differentially abundant transcripts (DATs, $p_{\text{adj}} < .05$) in day 9 versus day 7 and in day 12 versus day 9 blastocysts, respectively. DATs were categorized into eight different groups according to their gene expression pattern over the course of time, that is, steadily increasing or decreasing; peaking at day 7, 9, or 12; and showing no difference between day 7 and 9 but increase or decrease at day 12 and vice versa. Identified DATs were compared to gene sets, which have been reported to be specific for EPI, PE/HB, and TE in mouse, human, and bovine embryos (Figure 2, Data S1). Transcripts from EPI-specific genes were generally more prominent at day 7 and day 9 than at day 12; consistent with the proportion of *OCT4*-positive cells at day 7 and 9 (Figure 1), the abundance of *OCT4* transcripts steadily decreased until day 12. *NANOG* and *SOX2* mRNAs showed similar abundances at day 7 and 9 but decreased by day 12. *NODAL*, a member of the pluripotency maintaining TGF β /ACTIVIN/NODAL signaling pathway,¹⁵ increased 80-fold from day 7 to day 9 and again decreased 2.8-fold by day 12. Interestingly, the mRNA levels for the *NODAL* antagonist *LEFTY2*¹⁶ followed the same pattern, while the transcript levels of the *NODAL*-activating convertase *FURIN*¹³ steadily increased. The only EPI gene showing its highest transcript abundance at day 12 was *FGFR1*, which in pregastrulation stage human embryos were reported to be enriched in HB cells.¹⁷ HB-specific transcripts mostly increased until day 12, except *GATA6* and *HDAC1*. While the decreasing abundance of *GATA6* mRNA was consistent with the observed pattern in the immunofluorescence staining, *SOX17* mRNA was not differentially abundant between day 7 and day 9 but increased later at day 12. *CDX2* mRNA, encoding an early marker for TE, was not differentially abundant between day 7 and day 9 but increased 1.5-fold until day 12. Except group 2 (Figure 2), TE genes were present in every expression pattern, indicating that this lineage undergoes dynamic changes during the observed period.

A previously published global transcriptomic dataset covering in vitro cultured day 7 embryos from in vitro fertilization (IVP Ctrl) and SCNT with wild-type cells (NT Ctrl) or cells carrying an *OCT4* KO mutation (*OCT4*KO^{tm1})⁹ was reanalyzed using the current genome assembly ARS-UCD1.2¹⁸ and compared to the transcriptome profile of in vivo produced day 7 embryos. By comparing the DATs of the three above-mentioned groups against in vivo produced

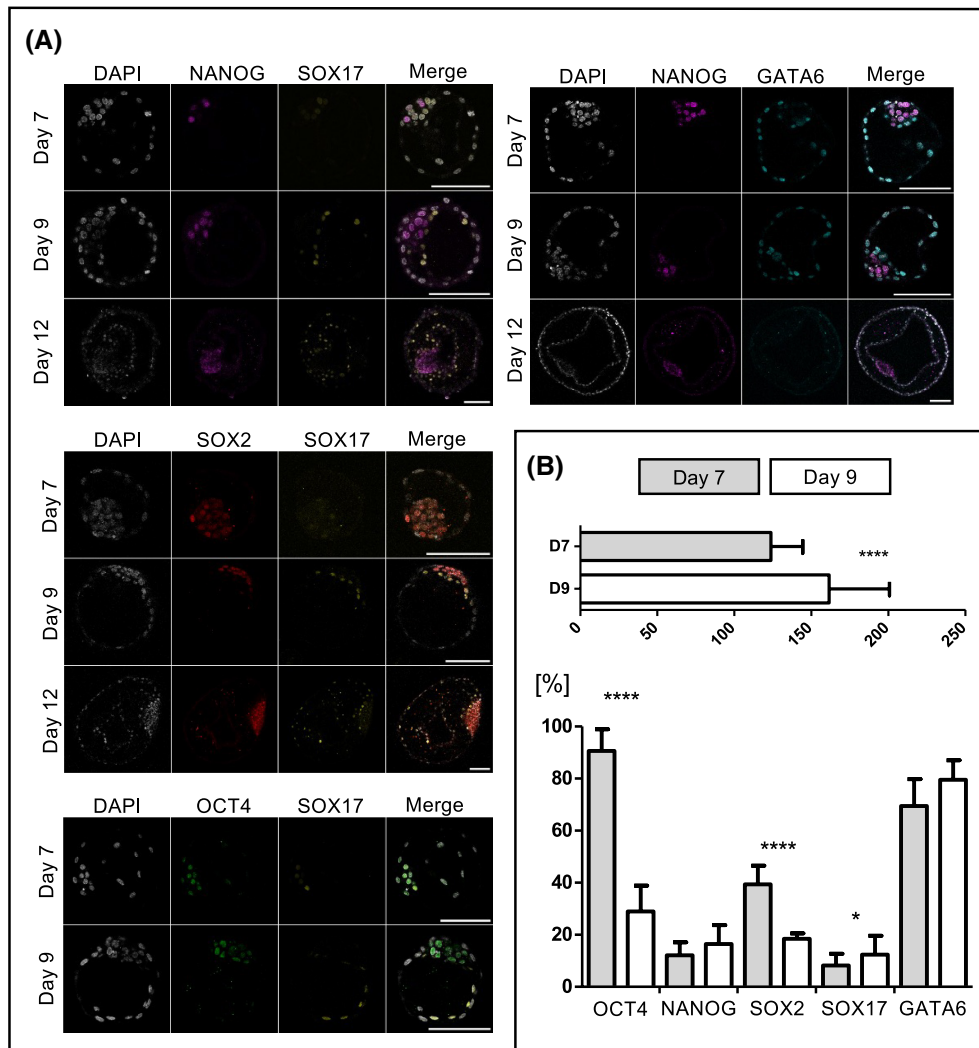


FIGURE 1 The second lineage differentiation in embryos produced in vivo. (A) Representative confocal planes of day 7, 9, and 12 embryos stained for NANOG/SOX17 ($n = 10, 5,$ and 5), NANOG/GATA6 ($n = 10, 6,$ and 3), SOX2/SOX17 ($n = 8, 6,$ and 4), and OCT4/SOX17 ($n = 10$ and 5). All scale bars represent $100 \mu\text{m}$. Note that the confocal plane shown for OCT4/SOX17 in the day 7 blastocyst was selected to show an SOX17-positive cell in the inner cell mass. While OCT4 in the trophectoderm is not clearly visible in this particular plane, it was consistently present in this lineage (Figure S1). (B) Total cell numbers and proportion of cells stained positive for lineage-specific markers at day 7 (D7) and day 9 (D9) relative to the total cell number. Data are presented as mean \pm SD, asterisks indicate significant differences between D7 and D9 (two-tailed t test, $*p < .05$; $****p < .0001$). Number of examined embryos: Total cell number (D7: $n = 44$; D9: $n = 21$), OCT4 (D7: $n = 10$; D9: $n = 5$), NANOG (D7: $n = 17$; D9: $n = 11$), SOX2 (D7: $n = 15$; D9: $n = 5$), SOX17 (D7: $n = 20$; D9: $n = 15$), GATA6 (D7: $n = 10$; D9: $n = 6$). Calculation of percentage of SOX17-positive cells does not include embryos with no SOX17 expression ($n = 8$)

day 7 embryos, we identified transcripts that were differentially abundant due to the SCNT procedure or in vitro culture. Five lineage-specific DATs appeared in all three groups and are therefore attributable to in vitro culture, causing reduced abundance of *HAND1* (TE) and *HDAC1* (HB) transcripts while mRNA levels of *HSD17B11* (EPI), *HMGCS1*, and *SLC2A3* (TE) were increased. Two DATs were specific to the SCNT procedure with increased levels of *CLDN7* (TE) transcripts and a lower mRNA abundance of *MAP2K6* (HB) (Figure S2A). The remaining lineage-specific DATs in *OCT4KO*^{tm1} against in vivo produced day 7 blastocysts included six, two, and three with decreased and one, five, and eight with increased levels from the EPI,

HB, and TE lineages, respectively (Figure S2B), showing a shift of gene expression toward the differentiated lineages TE and HB in the absence of OCT4.

3.2 | Induction of *OCT4* knockout without targeting a known *OCT4* pseudogene

Earlier studies on the function of OCT4 in bovine embryos^{9,19} used a sgRNA-sequence, which also targets an *OCT4* pseudogene present in intron 1 of *ETF1*.²⁰ Therefore, we adapted an sgRNA (sgRNA2b) known to be highly

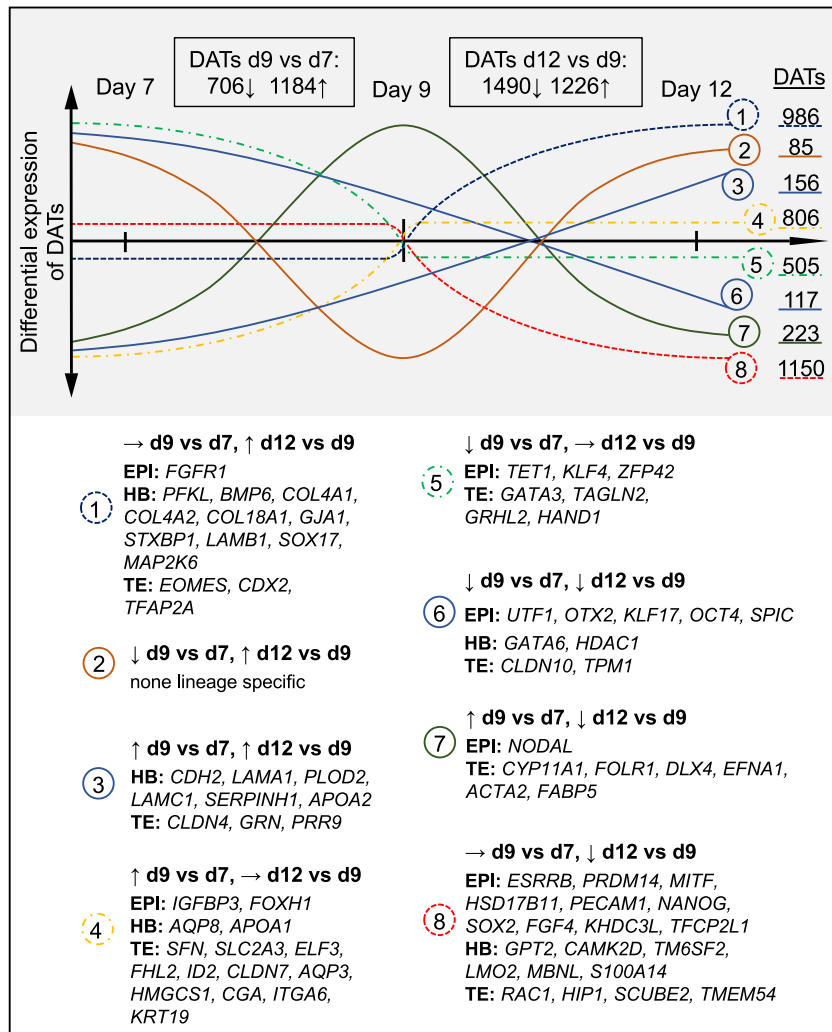


FIGURE 2 Differentially abundant transcripts (DATs) of in vivo produced blastocysts between day 7, 9, and 12 categorized into gene sets specific for epiblast (EPI), hypoblast (HB), and trophectoderm (TE). Three day 7 blastocysts and each four day 9 and 12 blastocysts were analyzed using DESeq2 ($p_{\text{adj}} < .05$)

efficient in human embryos²¹ to the bovine ortholog sequence, where it spans an exon–intron junction at the 3′-end of exon 2 and thus does not target the pseudogene in *ETF1*, because the retrocopy does not contain intronic *OCT4* sequences.²⁰ The sgRNA2b sequence was cloned into PX459 V2.0 to knock out *OCT4* in somatic cells and single-cell clones were produced after selection with puromycin.²² From 31 single-cell clones, three retained the wild-type sequence while 11 carried homozygous mutations that were confirmed by a single-nucleotide polymorphism 179 bp downstream the sgRNA2b cutting site. The remaining single-cell clones had bi-allelic heterozygous ($n = 13$) or mono-allelic ($n = 4$) mutations. None of the single-cell clones had any mutation at the *OCT4* pseudogene, showing that sgRNA2b specifically targets *OCT4*. From the same transfection experiment, two single-cell clones with the same homozygous deletion of two base pairs (*OCT4*^{2bKOX1} and *OCT4*^{2bKOX4}) and one where no mutation had occurred (NT Ctrl^{2b}) were used to reconstruct embryos via SCNT. Embryos from *OCT4*^{2bKOX1} developed to blastocysts by day 7, albeit at a much lower rate than NT Ctrl^{2b} embryos, while there was no difference between

OCT4^{2bKOX4} and NT Ctrl^{2b} (Table 1A). NT Ctrl^{2b} showed expression of OCT4 in both TE and ICM ($n = 4$), while blastocysts from *OCT4*^{2bKOX1} ($n = 5$) and *OCT4*^{2bKOX4} ($n = 6$) stained negative (Figure S3). By day 8, we observed that NT Ctrl^{2b} embryos had expanded and started hatching through the incision in the ZP made during the SCNT procedure, while *OCT4*^{2bKOX1} and *OCT4*^{2bKOX4} were not able to exit the ZP and expanded to a lesser extent compared to NT Ctrl^{2b} embryos.

3.3 | SOX17 is lost in blastocysts lacking OCT4

To elucidate the effects of loss of OCT4 during the second lineage differentiation, we performed immunofluorescent staining of the lineage-specific markers GATA6, SOX17, NANOG, and SOX2^{23,24} at day 8 blastocyst stage. In IVP Ctrl and NT Ctrl^{2b} embryos, we confirmed that at day 8, expression of SOX2 is restricted to the ICM and that NANOG and SOX17 are mutually exclusive markers of the EPI and HB, respectively. GATA6 is expressed in both ICM and TE, and

TABLE 1 Developmental rates of somatic cell nuclear transfer (SCNT) embryos

Experimental group	<i>OCT4</i> ^{2bKOX1}	<i>OCT4</i> ^{2bKOX4}	NT Ctrl ^{2b}
No. of SCNT experiments	7	4	9
No. of fused constructs	276	142	166
Cleavage rate* (%)	79.9 ± 11	83.5 ± 6.5	70.3 ± 15.5
Morula rate* (%)	42.7 ± 11.6	58.2 ± 7.7	47 ± 16.6
Blastocyst rate* (%)	15.1 ± 6.9 ^a	38.2 ± 3.7 ^b	40.4 ± 13.5 ^b

Note: Different superscript letters within a row indicate significant differences ($p < .05$, one-way ANOVA with Tukey multiple comparison test).

*Data presented as mean ± SD.

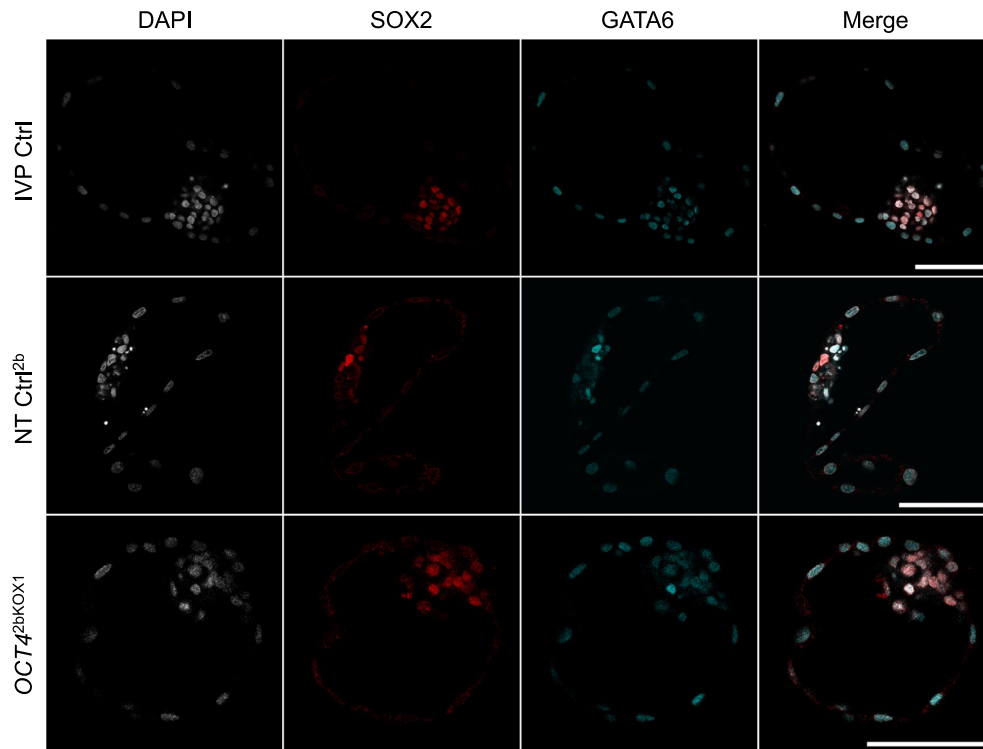


FIGURE 3 Expression of SOX2 and GATA6 in day 8 blastocysts. Representative confocal planes of IVP Ctrl, NT Ctrl, and *OCT4*^{2bKOX1} embryos stained for SOX2/GATA6 (each $n = 4$). All scale bars represent 100 μm

GATA6-negative cells are present in the ICM. In contrast to the expression pattern in day 9 in vivo produced embryos, SOX17 and GATA6 are always co-expressed with SOX2, indicating that SOX2 is a late EPI marker (Figure 3, Figures S4 and S5). In *OCT4*^{2bKOX1} day 8 SCNT blastocysts, there were no GATA6-negative cells and SOX2 was expressed exclusively in the ICM (Figure 3). As reported previously,⁹ there was no expression of NANOG and we did not detect any SOX17-positive cells (Figures S4 and S5).

To validate our findings from SCNT experiments, we induced KO of *OCT4* directly in zygotes from in vitro fertilization (IVF) by injection of a ribonucleoprotein (RNP) consisting of Cas9 protein and synthesized sgRNA2b. As control, we used an RNP with no target in the bovine genome (sgRNA Ctrl). Developmental data from 11 experiments with a total of 1224, 462, and 543 zygotes injected with *OCT4*^{2bZ1}, sgRNA Ctrl, or non-injected, respectively,

revealed that the injection procedure induced a decreased cleavage rate, but did not affect the percentage of blastocysts developed from cleaved zygotes (Table 2). To determine the mutation rate after injection, DNA was isolated from individual embryos and the targeted site was amplified for subsequent Sanger sequencing. From four experiments, we analyzed putative mutations in a total of 57 day 7 blastocysts, of which 34 had expanded. There were no significant differences in percentage of wild-type, biallelic, homozygous, or monoallelic mutations between expanded and early day 7 blastocysts (Figure 4D) and four expanded blastocysts carried homozygous mutations that induced a shift of the reading frame. Staining with antibodies against NANOG, SOX17, and *OCT4* in *OCT4*^{2bZ1} day 8 blastocysts in combination with genotyping after the imaging procedure enabled us to confirm the absence of *OCT4* on the protein level and frame shift mutation on

Experimental group	<i>OCT4</i> ^{2bZI}	sgRNA Ctrl	Non-injected
No. of ZI experiments	11		
No. of injected zygotes	1224	462	543
Cleavage rate* (%)	66.4 ± 10.5 ^a	68.3 ± 12.9 ^a	84 ± 5.4 ^b
Morula rate* (%)	36.9 ± 10.3 ^a	42.9 ± 8.8 ^a	56.8 ± 11.1 ^b
Blastocyst rate* (%)	21.7 ± 9.9 ^a	27.1 ± 11.1 ^{ab}	37.2 ± 5.9 ^b

Note: Different superscript letters within a row indicate significant differences ($p < .05$, one-way ANOVA with Tukey multiple comparison test).

*Data presented as mean ± SD.

TABLE 2 Developmental rates of in vitro fertilized embryos after zygote injection (ZI)

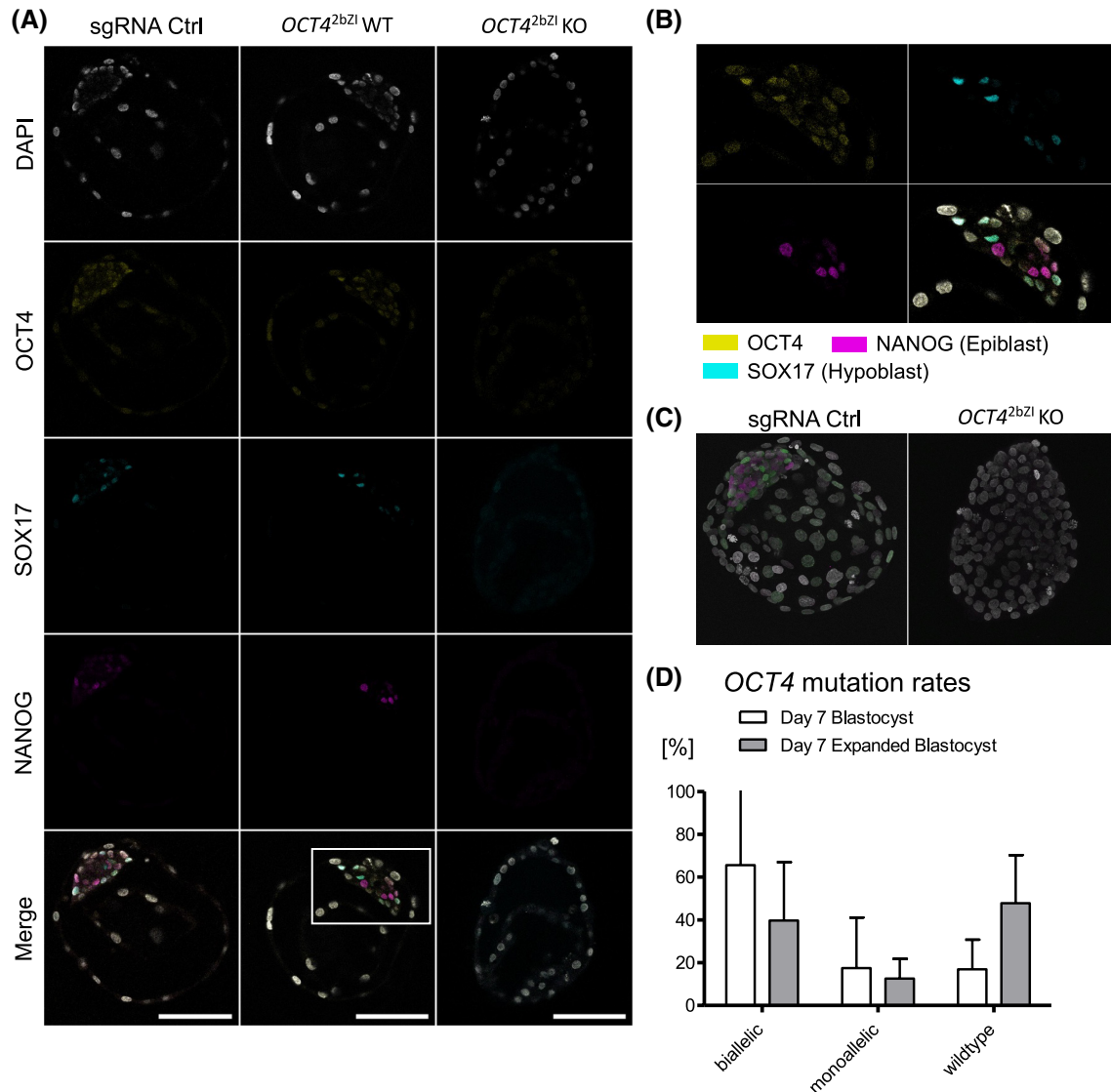


FIGURE 4 The effect of loss of *OCT4* in vitro fertilized embryos. (A) Representative confocal planes of day 8 blastocysts injected at zygote stage with a ribonucleoprotein without target (sgRNA Ctrl, $n = 8$) or targeting *OCT4* (sgRNA2b), where the wild-type genotype was maintained (*OCT4*^{2bZI} WT, $n = 3$) or knockout induced (*OCT4*^{2bZI} KO, $n = 11$). Scale bars represent 100 μm. (B) Enlarged region from panel (A) (*OCT4*^{2bZI} WT merge). (C) Three-dimensional projections of sgRNA Ctrl and *OCT4*^{2bZI} KO blastocysts from panel (A). (D) *OCT4* mutation rates in expanded and nonexpanded day 7 blastocysts ($p > .05$, two-tailed t test)

the genomic level in addition to the expression patterns of NANOG and SOX17. Blastocysts developing from zygotes injected with sgRNA Ctrl showed mutually exclusive

expression of NANOG and SOX17 and co-expression of both markers with *OCT4* ($n = 8$), while in *OCT4*^{2bZI} blastocysts with successful deletion of *OCT4*, both proteins

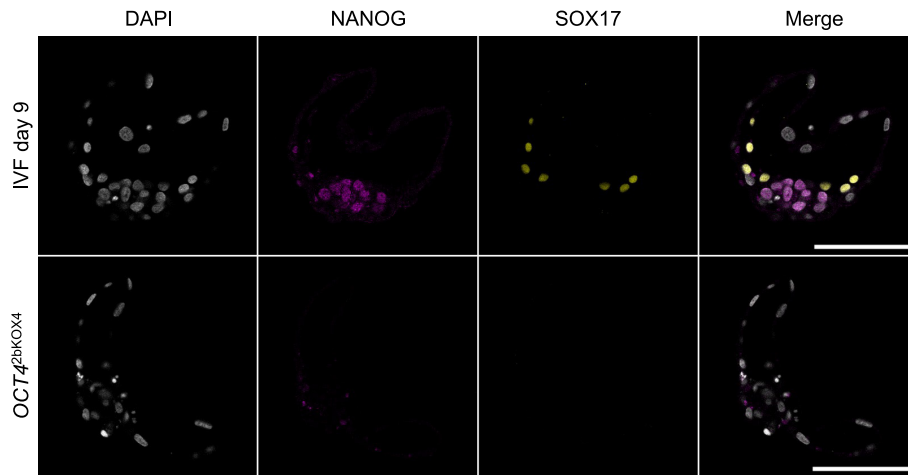


FIGURE 5 Day 9 expanded blastocysts collected from recipient heifers stained against NANOG and SOX17. Representative confocal planes of day 9 blastocysts transferred to a recipient at day 6 and collected at day 9 from in vitro fertilization (IVF) or produced by somatic cell nuclear transfer using *OCT4*^{2bKOX4} cells. Scale bars represent 100 μ m

could not be detected ($n = 11$, Figure 4A–C, Video S1 and S2). Developmental data from *OCT4* KO embryos produced by both SCNT and IVF show that *OCT4* is not essential for the formation of an expanded blastocyst by day 7. Expansion was present in SCNT embryos—although less pronounced—as well as in IVF embryos that carried biallelic *OCT4* frameshift mutations. Yet, a decreased blastocyst rate in *OCT4*^{2bKOX1} SCNT embryos and a higher percentage of expanded blastocysts in *OCT4*-intact embryos demonstrate that loss of *OCT4* impedes development to the expanded blastocyst stage.

3.4 | Uterine environment cannot rescue the second lineage differentiation in *OCT4* KO embryos

To evaluate if the phenotype of *OCT4* KO embryos as described above is alleviated or rescued when the second lineage differentiation occurs in utero, we transferred each four day 6 *OCT4*^{2bKOX4} early blastocysts to five synchronized heifers and collected the embryos at day 9. As controls, we used each four IVP Ctrl blastocysts transferred to two recipients. We collected three day 9 *OCT4*^{2bKOX4} expanded blastocysts from three different recipients and five IVP Ctrl expanded blastocysts. The transferred *OCT4*^{2bKOX4} and IVP Ctrl embryos showed total cell numbers similar to in vivo produced day 9 blastocysts (Figure 1B) with 139.3 ± 20.5 , 155.6 ± 50.28 , and 161.5 ± 39.1 cells, respectively (mean \pm SD, $p > .05$). Staining of NANOG and SOX17 revealed a similar expression pattern in IVF blastocysts compared to embryos completely developed in vivo. HB precursor cells began to form an inner lining within the blastocoel, which was confirmed by a similar proportion of SOX17-positive cells

(15.1 ± 5.8 vs. 18.9 ± 4.8 , mean [%] \pm SD, $p > .05$), while the proportion of NANOG-positive cells was markedly reduced in the IVF embryos (6.9 ± 3.8 vs. 16.5 ± 6.9 , mean [%] \pm SD, $p < .05$). All collected *OCT4*^{2bKOX4} blastocysts stained negative for NANOG and SOX17. Although we were not able to recover the majority of *OCT4*^{2bKOX4} blastocysts at day 9 (3/20), our data show that, in the absence of *OCT4*, bovine embryos survive until day 9 and expand in utero, but the second lineage differentiation cannot be rescued by a uterine environment (Figure 5).

3.5 | *OCT4* is required cell autonomously during the second lineage differentiation

We performed a chimera aggregation experiment in order to investigate, if *OCT4* is required cell-autonomously for the expression of NANOG and SOX17. Using fetal somatic cells (FSCs), we produced a single-cell clone, in which an eGFP expression vector was randomly integrated and *OCT4* was knocked out by homozygous deletion of two nucleotides in frame (*OCT4*^{2bKOeGFP}). Embryos from *OCT4*^{2bKOeGFP} developed to expanded day 8 blastocysts, ubiquitously expressed eGFP, and lacked expression of *OCT4* ($n = 7$), NANOG ($n = 8$), and SOX17 ($n = 7$). As aggregation partner, we used embryos generated from wild-type FSCs (NT Ctrl^{FSC}), which at day 8 expressed SOX17 and NANOG as expected ($n = 3$, Figure 6, Figure S6). In three experiments, we aggregated 25 chimeras and 12 showed contribution of both *OCT4*^{2bKOeGFP} and NT Ctrl^{FSC} cells to the blastocyst. In none of these chimeras, we detected co-expression of eGFP with NANOG or SOX17 (Figure 6). Therefore, we conclude that *OCT4* expression in neighboring cells within the ICM cannot rescue NANOG or SOX17 expression.

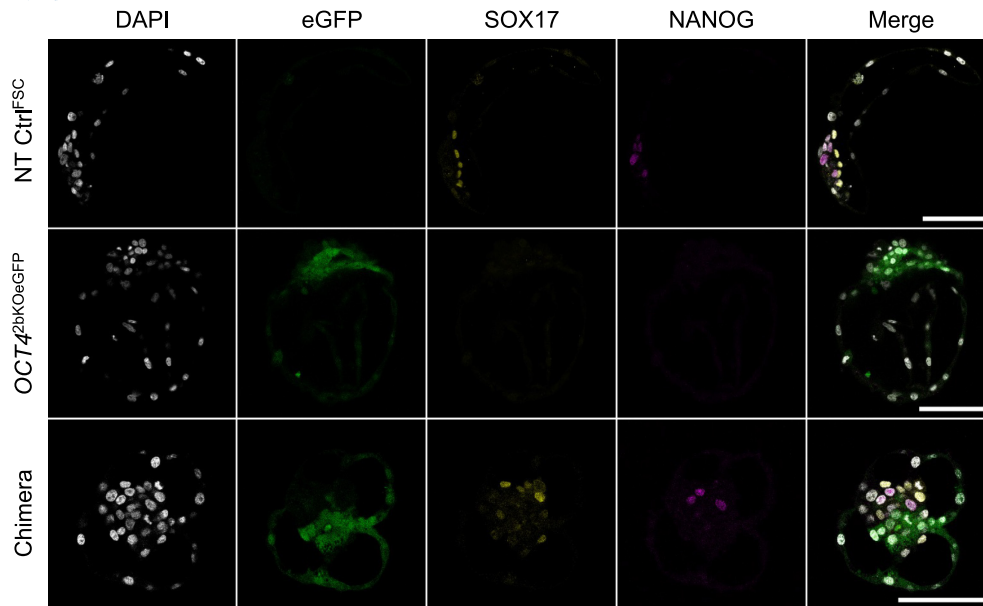


FIGURE 6 Chimera from wild-type and *OCT4* KO embryos. Representative confocal planes of day 8 blastocysts from somatic cell nuclear transfer using wild-type cells (NT Ctrl^{FSC}, $n = 3$) or cells tagged with eGFP carrying an *OCT4* KO mutation (*OCT4*^{2bKOeGFP}, $n = 7$) stained for NANOG and SOX17. Lower row in the panel shows chimera of the former embryos at day 8. Scale bars represent 100 μm

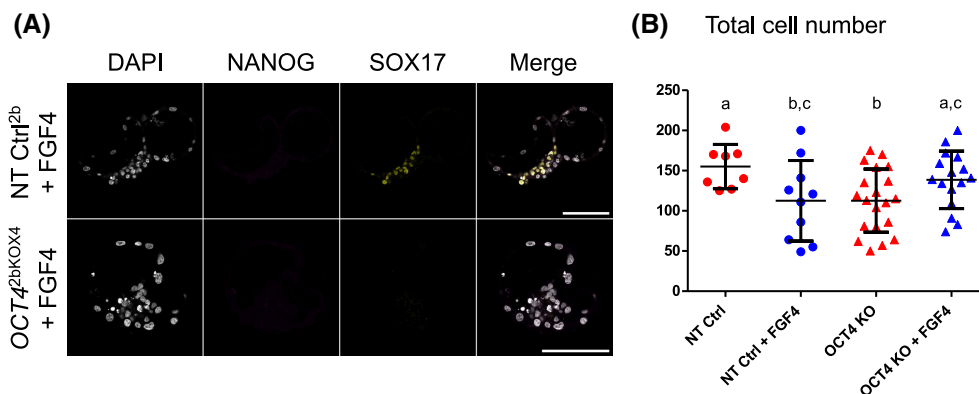


FIGURE 7 The effect of exogenous FGF4 on *OCT4* KO embryos. (A) Representative confocal planes of NT Ctrl^{2b} and *OCT4*^{2bKOX4} day 8 blastocysts treated with FGF4 and heparin, stained for NANOG/SOX17 (each $n = 10$). All scale bars represent 100 μm . (B) Total cell numbers of NT Ctrl^{2b} and *OCT4*^{2bKOX4} with or without FGF4 treatment. Different superscript letters indicate significant differences ($p < .05$, two-tailed t test)

To further elucidate the role of *OCT4* in the differentiation of the HB, we incubated *OCT4*^{2bKOX4} and NT Ctrl^{2b} with exogenous FGF4, which induces pan-ICM expression of HB-markers and ablates the expression of NANOG in wild-type embryos.²⁵ NT Ctrl^{2b} day 8 blastocysts showed full expression of SOX17 and no NANOG ($n = 10$), while in *OCT4*^{2bKOX4}, 10 of 16 blastocysts showed no expression of NANOG or SOX17 (Figure 7A). In two blastocysts, we found ectopic SOX17 expression in the TE and four blastocysts had positive cells in the ICM, albeit at a significantly lower proportion to the total cell number as FGF4 treated NT Ctrl^{2b} blastocysts (5 ± 2.4 vs. 16.3 ± 7.6 , mean [%] \pm SD, $p < .05$) and with a lower intensity of the fluorescent signal (Figure S7). Pairwise comparisons of the total cell number revealed a significant reduction due

to loss of *OCT4*, which was alleviated by exogenous FGF4, while in NT Ctrl^{2b} blastocysts, FGF4 had a detrimental effect on the total cell number (Figure 7B). Because neither chimeric complementation nor treatment with exogenous FGF4 could restore a failing differentiation of the HB in cells without functional *OCT4*, we conclude that *OCT4* is required cell autonomously to induce HB formation.

4 | DISCUSSION

In this study, we set out to further elucidate the role of *OCT4* in bovine preimplantation development, especially during the second lineage differentiation. Because it has

not been entirely clear how the expression of known markers of the different lineages evolves during the establishment of the HB lineage, we examined the patterns in embryos produced *in vivo* at the blastocyst stage (day 7), the expanded blastocyst stage (day 9), and the ovoid blastocyst stage (day 12). Complete HB migration by day 11 has been documented before by staining of SOX17.²⁶ We were able to show, that said migration begins at day 9 with an increase of SOX17 cells, which organize into the visceral HB and end the salt and pepper distribution of HB- and EPI-precursor cells within the ICM. Interestingly, despite an increase in SOX17 cell numbers between day 7 and day 9, we did not detect differences in SOX17 transcript abundance. At day 7, we found a subset of embryos where SOX17 was not present yet, while in embryos that expressed the marker, intensity was low, mutually exclusive with NANOG and restricted to the ICM. Other studies using *in vitro* produced embryos report co-expression of SOX17 with NANOG as early as the 16–32 cell stage¹⁰ and ectopic expression in the TE until day 6.5.²⁷ In contrast to various reports using *in vitro* produced embryos,^{9,10,25} we did not find co-expression of GATA6 and NANOG in day 7 *in vivo* produced embryos, indicating an earlier commitment to the HB or EPI lineage by reciprocal repression. The pluripotency factors OCT4 and SOX2 are restricted to the EPI by day 9, while at day 7, they are expressed throughout the blastocyst or the ICM, respectively, confirming SOX2 as a reliable marker for the ICM at day 7.²⁴ While OCT4 is not clearly visible in the TE of the day 7 blastocyst shown in Figure 1 (due to the selection of a confocal plain that provides optimal representation of SOX17), it was consistently present in this lineage in both day 7 *in vivo* produced (Figure S1) and SCNT blastocysts (Figure S3). The expression patterns described here may serve as a benchmark for assessing the quality of bovine embryos from long-term culture systems.²⁶ *In vitro* produced controls, that were transferred to recipients at day 6 and flushed at day 9, displayed the same total cell number and SOX17/NANOG expression pattern as embryos produced *in vivo*, showing that short-term incubation *in vivo* is sufficient for stage-adequate development of the embryo, as reported previously.²⁸

Consistent with the staining pattern and in line with a previous report, we observed a steady reduction of OCT4 transcripts from day 7 to day 12, while the abundance of NANOG and SOX2 transcripts did not change between day 7 and day 9 and eventually decreased by day 12.²⁹ Similar to human pregastrulation development, we found a decreasing abundance of transcripts associated with naïve pluripotency (*KLF4*, *KLF17*, *PRDM8*, *TFCP2L1*, *ZFP42*, *UTF1*), while markers for primed pluripotency, that increased in human (*FGF2*, *DNMT3B*, *SOX11*, *SFRP2*, *SALL2*),¹⁷ did not change from day 7 until day 12. Van

Leeuwen et al¹³ detected *NODAL* transcripts in the EPI of Rauber's layer (RL) stage (day 10–11) embryos and suggested *NODAL* activation through the convertase *FURIN*, which they detected in the RL. We found a massive increase (80-fold) in *NODAL* transcripts between day 7 and 9 together with an increase of *FURIN* and *LEFTY2* mRNAs, indicating that the *NODAL/BMP/WNT* pathway, that later regulates patterning,³⁰ is already activated by day 9. Comparing transcriptome profiles from day 7, 9, and 12 *in vivo* produced embryos enabled analysis of the dynamics of lineage-specific expression patterns during bovine development. Nevertheless, a greater sample size is still required to ultimately identify the stage-specific expression profiles at these respective stages.

Studies on the effects of *in vitro* culture on the transcriptome of bovine blastocysts have mainly identified pathways related to “energetic metabolism, extracellular matrix remodeling, and inflammatory signaling”.³¹ While we found a total of 463 DATs between *in vivo* and *in vitro* produced day 7 embryos, only five DATs were lineage specific, indicating that the *in vitro* culture system has no substantial effect on the mechanisms of lineage differentiation. The fact that we only found two lineage-specific DATs between NT Ctrl and *in vivo* produced embryos strengthens the use of embryos from SCNT to study the basic mechanisms of early lineage differentiation.

By generating *OCT4* KO embryos with an sgRNA that exclusively targets *OCT4* using both SCNT and ZI, we aimed to resolve existing conflicts regarding the *OCT4* KO phenotype in bovine embryos. We confirmed that, regardless of the applied method, *OCT4* is not essential for the expansion of the blastocyst and showed that *OCT4* KO embryos survive until day 9 when transferred to a recipient cow. Daigneault et al¹⁹ reported that targeting *OCT4* using ZI prevented development to the expanded blastocyst stage, while a previous report from our laboratory showed an unchanged morphology of *OCT4* KO blastocysts.⁹ These two studies used the same sgRNA sequence, which also targets the pseudogene present in *ETF1*; therefore, it is unlikely that off-target effects caused the divergent phenotypes. Here, we also applied ZI to delete *OCT4* and observed expansion of the blastocysts; therefore, we can exclude the effects of the different procedures used to knock out *OCT4*. We can only speculate that the conflicting results are caused by variables in the ZI procedure or the *in vitro* culture system.

As reported previously,⁹ loss of NANOG was observed in all embryos without functional *OCT4*, but the pluripotency marker *SOX2* was independent of *OCT4*, as reported previously¹⁹ and similar to mouse embryos.⁷ Although there was no reduction in expression of the early HB marker *GATA6*, expression of *SOX17* failed in the absence of *OCT4*. As expression of *SOX17* is not dependent

on NANOG,³² loss of SOX17 can be linked directly to the OCT4 KO phenotype. In mouse embryos, *Oct4* KO prevents the differentiation of the PE, not only because FGF4-MEK signaling is reduced³³ but also because OCT4 is required cell autonomously.^{7,8} Nevertheless, Frum et al⁷ reported a modest induction of PE gene expression upon treatment with FGF4 in *Oct4* KO mouse embryos, indicating that an alternative OCT4-independent pathway exists. We observed faint expression of SOX17 in a subset of *OCT4* KO embryos treated with FGF4, which might be explained by such a pathway, but full expression of SOX17 was only possible when OCT4 was present. Using chimeric complementation, we were able to show that paracrine factors produced by *OCT4* intact cells are not sufficient to restore the OCT4 deficiency. Therefore, and similar to mouse, the development of the HB requires OCT4 not only to produce paracrine factors, for example, FGF4, but also for the induction of differentiation in HB precursor cells, that is, OCT4 is required cell autonomously.

In conclusion, our data show that in the bovine preimplantation embryo OCT4 is required during the second lineage differentiation for the maintenance of pluripotency in the EPI and differentiation of the HB.

ACKNOWLEDGMENTS

We thank Eva-Maria Hinrichs, Tuna Güngör, and Maximilian Moraw for their excellent technical assistance and Christophe Jung for access to confocal laser scanning microscopy in the Center for Advanced Light Microscopy (CALM), LMU Munich. This work was supported by funds from the Deutsche Forschungsgemeinschaft (DFG) under grants 405453332 and TRR127 and the Bayerische Forschungsförderung under grant AZ-1300-17.

DISCLOSURES

The authors declare no competing interests.

AUTHOR CONTRIBUTIONS

KS analyzed the data and prepared the initial draft. KS, MK, VZ, HDR, CS, AB, and JPM designed and performed experiments. MK, VZ, HDR, HB, and EW contributed to the writing of the manuscript. KS and EW acquired funding.

DATA AVAILABILITY STATEMENT

The data that support the findings of this study are available in the methods and/or supplementary material of this article.

ORCID

Kilian Simmet  <https://orcid.org/0000-0003-2188-3108>
 Eckhard Wolf  <https://orcid.org/0000-0002-0430-9510>

REFERENCES

1. Artus J, Chazaud C. A close look at the mammalian blastocyst: epiblast and primitive endoderm formation. *Cell Mol Life Sci.* 2014;71:3327-3338.
2. Chazaud C, Yamanaka Y. Lineage specification in the mouse preimplantation embryo. *Development.* 2016;143:1063-1074.
3. Simmet K, Zakhartchenko V, Wolf E. Comparative aspects of early lineage specification events in mammalian embryos—insights from reverse genetics studies. *Cell Cycle.* 2018;17(14):1688-1695.
4. Springer C, Wolf E, Simmet K. A new toolbox in experimental embryology—alternative model organisms for studying preimplantation development. *J Dev Biol.* 2021;9:15.
5. Gerri C, Menchero S, Mahadevaiah SK, Turner JM, Niakan KK. Human embryogenesis: a comparative perspective. *Annu Rev Cell Dev Biol.* 2020;36:411-440.
6. Frum T, Ralston A. Cell signaling and transcription factors regulating cell fate during formation of the mouse blastocyst. *Trends Genet.* 2015;31:402-410.
7. Frum T, Halbisen MA, Wang C, Amiri H, Robson P, Ralston A. Oct4 cell-autonomously promotes primitive endoderm development in the mouse blastocyst. *Dev Cell.* 2013;25:610-622.
8. Le Bin GC, Muñoz-Descalzo S, Kurowski A, et al. Oct4 is required for lineage priming in the developing inner cell mass of the mouse blastocyst. *Development.* 2014;141:1001-1010.
9. Simmet K, Zakhartchenko V, Philippou-Massier J, Blum H, Klymiuk N, Wolf E. OCT4/POU5F1 is required for NANOG expression in bovine blastocysts. *Proc Natl Acad Sci USA.* 2018;115:2770-2775.
10. Canizo JR, Rivolta AEY, Echegaray CV, et al. A dose-dependent response to MEK inhibition determines hypoblast fate in bovine embryos. *BMC Dev Biol.* 2019;19:13.
11. Bernardo AS, Jouneau A, Marks H, et al. Mammalian embryo comparison identifies novel pluripotency genes associated with the naïve or primed state. *Biol Open.* 2018;7:bio033282. [10.1242/bio.033282](https://doi.org/10.1242/bio.033282)
12. Charpigny G, Marquant-Le Guenne B, Richard C, et al. PGE2 supplementation of oocyte culture media improves the developmental and cryotolerance performance of bovine blastocysts derived from a serum-free in vitro production system, mirroring the inner cell mass transcriptome. *Front Cell Dev Biol.* 2021;9:672948.
13. van Leeuwen J, Berg DK, Pfeffer PL. Morphological and gene expression changes in cattle embryos from hatched blastocyst to early gastrulation stages after transfer of in vitro produced embryos. *PLoS One.* 2015;10:e0129787.
14. Pfeffer PL, Smith CS, Maclean P, Berg DK. Gene expression analysis of bovine embryonic disc, trophoblast and parietal hypoblast at the start of gastrulation. *Zygote.* 2017;25:265-278.
15. Papanayotou C, Collignon J. Activin/Nodal signalling before implantation: setting the stage for embryo patterning. *Philos Trans R Soc Lond B Biol Sci.* 2014;369:20130539.
16. Hill CS. Spatial and temporal control of NODAL signaling. *Curr Opin Cell Biol.* 2018;51:50-57.
17. Molè MA, Coorens THH, Shahbazi MN, et al. A single cell characterisation of human embryogenesis identifies pluripotency transitions and putative anterior hypoblast centre. *Nat Commun.* 2021;12:3679.
18. Rosen BD, Bickhart DM, Schnabel RD, et al. De novo assembly of the cattle reference genome with single-molecule sequencing. *GigaScience.* 2020;9. [10.1093/gigascience/giaa021](https://doi.org/10.1093/gigascience/giaa021)

19. Daigneault BW, Rajput S, Smith GW, Ross PJ. Embryonic POU5F1 is required for expanded bovine blastocyst formation. *Sci Rep*. 2018;8:7753.
20. Schiffmacher AT, Keefer CL. CDX2 regulates multiple trophoblast genes in bovine trophoblast CT-1 cells. *Mol Reprod Dev*. 2013;80:826-839.
21. Fogarty NM, McCarthy A, Snijders KE, et al. Genome editing reveals a role for OCT4 in human embryogenesis. *Nature*. 2017;550:67.
22. Ran FA, Hsu PD, Wright J, Agarwala V, Scott DA, Zhang F. Genome engineering using the CRISPR-Cas9 system. *Nat Protoc*. 2013;8:2281-2308.
23. Khan DR, Dubé D, Gall L, et al. Expression of pluripotency master regulators during two key developmental transitions: EGA and early lineage specification in the bovine embryo. *PLoS One*. 2012;7:e34110.
24. Goissis MD, Cibelli JB. Functional characterization of SOX2 in bovine preimplantation embryos. *Biol Reprod*. 2014;90(2):30.
25. Kuijk EW, van Tol LT, Van de Velde H, et al. The roles of FGF and MAP kinase signaling in the segregation of the epiblast and hypoblast cell lineages in bovine and human embryos. *Development*. 2012;139:871-882.
26. Ramos-Ibeas P, Lamas-Toranzo I, Martínez-Moro Á, et al. Embryonic disc formation following post-hatching bovine embryo development in vitro. *Reproduction*. 2020;160:579-589.
27. Kohri N, Akizawa H, Iisaka S, et al. Trophoblast regeneration to support full-term development in the inner cell mass isolated from bovine blastocyst. *J Biol Chem*. 2019;294:19209-19223.
28. Machado GM, Ferreira AR, Pivato I, et al. Post-hatching development of in vitro bovine embryos from day 7 to 14 in vivo versus in vitro. *Mol Reprod Dev*. 2013;80:936-947.
29. Velásquez A, Veraguas D, Cabezas J, Manríquez J, Castro F, Rodríguez-Alvarez L. The expression level of SOX2 at the blastocyst stage regulates the developmental capacity of bovine embryos up to day-13 of in vitro culture. *Zygote*. 2019;27:398-404.
30. van Leeuwen J, Rawson P, Berg DK, Wells DN, Pfeffer PL. On the enigmatic disappearance of Rauber's layer. *Proc Natl Acad Sci USA*. 2020;117:16409-16417.
31. Cagnone G, Sirard M-A. The embryonic stress response to in vitro culture: insight from genomic analysis. *Reproduction*. 2016;152:R247-R261.
32. Springer C, Zakhartchenko V, Wolf E, Simmet K. Hypoblast formation in bovine embryos does not depend on NANOG. *Cells*. 2021;10:2232.
33. Nichols J, Zevnik B, Anastassiadis K, et al. Formation of pluripotent stem cells in the mammalian embryo depends on the POU transcription factor Oct4. *Cell*. 1998;95:379-391.
34. Reichenbach M, Lim T, Reichenbach H-D, et al. Germ-line transmission of lentiviral PGK-EGFP integrants in transgenic cattle: new perspectives for experimental embryology. *Transgenic Res*. 2010;19:549-556.
35. Klein C, Bauersachs S, Ulbrich SE, et al. Monozygotic twin model reveals novel embryo-induced transcriptome changes of bovine endometrium in the preattachment period. *Biol Reprod*. 2006;74:253-264.
36. Dobin A, Gingeras TR. Mapping RNA-seq reads with STAR. *Curr Protoc Bioinformatics*. 2015;51:11.14.11-11.14.19. [10.1002/0471250953.bi1114s1](https://doi.org/10.1002/0471250953.bi1114s1)
37. Love MI, Huber W, Anders S. Moderated estimation of fold change and dispersion for RNA-seq data with DESeq2. *Genome Biol*. 2014;15:550.
38. Babicki S, Arndt D, Marcu A, et al. Heatmapper: web-enabled heat mapping for all. *Nucleic Acids Res*. 2016;44:W147-W153.
39. Bauersachs S, Ulbrich SE, Zakhartchenko V, et al. The endometrium responds differently to cloned versus fertilized embryos. *Proc Natl Acad Sci USA*. 2009;106:5681-5686.
40. Simmet K, Reichenbach M, Reichenbach H-D, Wolf E. Phytohemagglutinin facilitates the aggregation of blastomere pairs from day 5 donor embryos with day 4 host embryos for chimeric bovine embryo multiplication. *Theriogenology*. 2015;84:1603-1610.
41. Messinger SM, Albertini DF. Centrosome and microtubule dynamics during meiotic progression in the mouse oocyte. *J Cell Sci*. 1991;100:289-298.
42. Wuensch A, Habermann FA, Kurosaka S, et al. Quantitative monitoring of pluripotency gene activation after somatic cloning in cattle. *Biol Reprod*. 2007;76:983-991.
43. de Chaumont F, Dallongeville S, Chenouard N, et al. Icy: an open bioimage informatics platform for extended reproducible research. *Nat Methods*. 2012;9:690-696.
44. Mutterer J, Zinck E. Quick-and-clean article figures with FigureJ. *J Microsc*. 2013;252:89-91.
45. Vochozkova P, Simmet K, Jemiller EM, Wunsch A, Klymiuk N. Gene editing in primary cells of cattle and pig. *Methods Mol Biol*. 2019;1961:271-289.
46. Hedegaard C, Kjaer-Sorensen K, Madsen LB, et al. Porcine synapsin 1: SYN1 gene analysis and functional characterization of the promoter. *FEBS Open Bio*. 2013;3:411-420.

SUPPORTING INFORMATION

Additional supporting information may be found in the online version of the article at the publisher's website.

How to cite this article: Simmet K, Kurome M, Zakhartchenko V, et al. OCT4/POU5F1 is indispensable for the lineage differentiation of the inner cell mass in bovine embryos. *FASEB J*. 2022;36:e22337. doi:[10.1096/fj.202101713RRR](https://doi.org/10.1096/fj.202101713RRR)